The Nucleocapsid Protein of Coronavirus Mouse Hepatitis Virus Interacts with the Cellular Heterogeneous Nuclear Ribonucleoprotein A1 *in Vitro* and *in Vivo*

Yicheng Wang and Xuming Zhang[1]

Department of Microbiology and Immunology, University of Arkansas for Medical Sciences, Little Rock, Arkansas 72205

Received May 28, 1999; returned to author for revision July 20, 1999; accepted September 28, 1999

The nucleocapsid (N) protein of mouse hepatitis virus (MHV) and the cellular heterogeneous nuclear ribonucleoprotein A1 (hnRNP-A1) are RNA-binding proteins, binding to the leader RNA and the intergenic sequence of MHV negative-strand template RNAs, respectively. Previous studies have suggested a role for both N and hnRNP-A1 proteins in MHV RNA synthesis. However, it is not known whether the two proteins can interact with each other. Here we employed a series of methods to determine their interactions both *in vitro* and *in vivo*. Both N and hnRNP-A1 genes were cloned and expressed in *Escherichia coli* as glutathione *S*-transferase (GST) fusion proteins, and their interactions were determined with a GST-binding assay. Results showed that N protein directly and specifically interacted with hnRNP-A1 *in vitro*. To dissect the protein-binding domain on the N protein, 15 deletion constructs were made by PCR and expressed as GST fusion proteins. Two hnRNP-A1-binding sites were identified on N protein: site A is located at amino acids 1 to 292 and site B at amino acids 392 to 455. In addition, we found that N protein interacted with itself and that the self-interacting domain coincided with site A but not with site B. Using a fluorescence double-staining technique, we showed that N protein colocalized with hnRNP-A1 in the cytoplasm, particularly in the perinuclear region, of MHV-infected cells, where viral RNA replication/transcription occurs. The N protein and hnRNP-A1 were coimmunoprecipitated from the lysates of MHV-infected cells either by an N- or by an hnRNP-A1-specific monoclonal antibody, indicating a physical interaction between N and hnRNP-A1 proteins. Furthermore, using the yeast two-hybrid system, we showed that N protein interacted with hnRNP-A1 *in vivo*. These results thus establish that MHV N protein interacts with hnRNP-A1 both *in vitro* and *in vivo*. © 1999 Academic Press

INTRODUCTION

Mouse hepatitis virus (MHV), a prototype of murine coronavirus, is a member of the *Coronaviridae* family. MHV contains a single-strand, positive-sense RNA genome of 31 kb in length (Pachuk *et al.,* 1989; Lee *et al.,* 1991; Lai and Cavanagh, 1997). Upon infection, the viral genomic RNA serves as a template for synthesis of a negative-strand, genome-length RNA, which in turn serves as a template for synthesis of six to seven subgenomic mRNAs (Lai and Cavanagh, 1997, and references therein). Each subgenomic mRNA contains a leader RNA of 72–77 nucleotides in length at the 5′-end, which is identical to the genomic RNA leader (Lai *et al.,* 1983, 1984). Depending on virus strains, there are two to four UCUAA repeats at the 3′-end of the leader, with the last repeat being UCUAAAC (Makino and Lai, 1989). An identical consensus UCUAAAC or similar sequence is present between each gene, termed intergenic (IG) sequence (Budzilowicz *et al.,* 1985; Shieh *et al.,* 1989), which serves as a joining point between the leader and

the body of a subgenomic mRNA. These subgenomic mRNAs are co-nested at the 3′-end. Double-stranded replicative-form RNAs and subgenomic negative-stranded RNAs complementary to each subgenomic mRNA are also found in infected cells (Sethna *et al.,* 1989; Sawicki and Sawicki, 1990). It has been suggested that the subgenomic minus-stranded RNAs might be first synthesized from the full-length genomic RNA template during initial transcription and that they subsequently serve as templates for synthesis of subgenomic mRNAs (Sawicki and Sawicki, 1995).

The precise mechanism(s) of MHV RNA transcription, however, remains elusive. Based on the structural features of the leader–body joining site of each subgenomic mRNA and the sequence complementarity between the 3′-end of the leader (5′-UCUAAAC-3′) and the consensus IG sequence of the negative-strand template (3′-AGAUUUG-5′), the leader-primed transcription model was proposed to explain how the leader RNA joins to the IG sequence to initiate subgenomic mRNA transcription (Lai *et al.,* 1983; Spaan *et al.,* 1983; Baric *et al.,* 1985). A number of subsequent experimental findings are compatible with this model (Lai and Cavanagh, 1997, and references therein). Using a mutant MHV, JHM2c, however, we previously found that a subgenomic mRNA species (mRNA2-1) can be initiated at a site other than the authentic UAAUAAAC sequence, where there is no

[1] To whom correspondence and reprint requests should be addressed at Department of Microbiology and Immunology, University of Arkansas for Medical Sciences, 4301 W. Markham Street, Slot 511, Little Rock, AR 72205. Fax: (501) 686-5359. E-mail: zhangxuming@exchange.uams.edu.

sequence complementarity between the leader and the template IG region (Zhang and Lai, 1994). This kind of mRNA initiation was also observed in a recombinant MHV A59 expressing a green fluorescence protein (Fisher et al., 1997). To explain how the leader joins to the IG region without sequence complementarity between them, we proposed that both the leader RNA and the IG sequence of the template may first interact with some cellular and/or viral proteins through protein–RNA interactions and that these two RNA elements are then brought together through protein–protein interactions to form a transcription initiation complex (Zhang et al., 1994b; Zhang and Lai, 1994). Subsequently, using UV cross-linking and gel retardation assays, we and others have identified some cellular proteins that specifically interact with the cis-acting sequences of MHV RNA (Furuya and Lai, 1993; Yu and Leibowitz, 1995; Zhang and Lai, 1995; Li et al., 1997, 1999).

One of the cellular RNA-binding proteins has been identified as heterogeneous nuclear ribonucleoprotein A1 (hnRNP-A1) (Li et al., 1997). hnRNP-A1 binds to the negative-strand leader and IG sequences, particularly the consensus (3'-AGAUUUG-5') sequence of MHV RNA. Site-directed mutagenesis analysis of the IG consensus sequence further suggests a role of hnRNP-A1 in MHV transcriptional regulation (Zhang and Lai, 1995). Although hnRNP-A1 is a nuclear protein, it relocalizes from the nucleus to the cytoplasm during MHV infection; this intracellular relocalization appears to be specific for hnRNP-A1 because another nuclear protein, Sam68, which has been shown to be relocalized to the cytoplasm during poliovirus infection (McBride et al., 1996), remains in the nucleus of MHV-infected cells (Li et al., 1997). These findings suggest that there is a physical and possibly functional link between hnRNP-A1 and MHV RNA replication and transcription apparatus (Li et al., 1997; Lai, 1998). Furthermore, direct evidence for a functional role for hnRNP-A1 in MHV RNA synthesis has been recently demonstrated in MHV-infected cells (Zhang et al., manuscript in preparation). On the other hand, the nucleocapsid (N) protein of MHV has been shown to bind to the UCUAAAC sequence of the leader RNA (Baric et al., 1988; Stohlman et al., 1988). It has thus been suggested that N protein is involved in MHV RNA transcription (Baric et al., 1988; Stohlman et al., 1988). The role of N protein in MHV RNA replication has also been demonstrated in an in vitro replication system (Compton et al., 1987). These findings suggest that both cellular hnRNP-A1 protein and viral N protein are components of the MHV replication and transcription complex. However, it is not known whether they can interact with each other. Since hnRNP-A1 interacts with some serine–arginine (SR)-rich proteins (Cartegni et al., 1996), and since N protein also contains an SR motif (Peng et al., 1995), it is conceivable that hnRNP-A1 may interact directly with N protein to bring the leader RNA to the IG

sequence of the template RNA for initiation of subgenomic mRNA transcription.

In this study, we thus explored this possibility by directly testing whether hnRNP-A1 directly interacts with MHV N protein in vitro and in vivo. We have expressed both hnRNP-A1 and N genes as glutathione S-transferase (GST)–fusion proteins and determined their interactions by a GST-binding assay. Results showed that hnRNP-A1 directly interacted with N protein in vitro. Using a fluorescence double-staining technique, we found that hnRNP-A1 colocalized with N protein in the perinuclear region of MHV-infected cells. Immunoprecipitation further demonstrated a physical interaction between hnRNP-A1 and N proteins in virus-infected cells. Furthermore, we found that hnRNP-A1 interacted with N protein in a yeast two-hybrid system. These studies thus establish that coronavirus N protein has a protein-binding activity and that it interacts with a cellular component of the putative MHV replication and transcription complex both in vitro and in vivo.

RESULTS

N protein interacts with hnRNP-A1 in vitro

To establish that N protein has protein-binding properties and that it can interact directly with hnRNP-A1, we cloned hnRNP-A1 and MHV N genes into pBluescript vectors for in vitro transcription and translation and into pGEX4-1 vectors for expression of GST fusion proteins. Their interactions were then determined by a GST-binding assay, in which one of the interacting partners is a GST fusion protein that was immobilized on the glutathione–Sepharose beads and the other was radiolabeled with [^{35}S]methionine in an in vitro translation reaction. When the GST–N fusion protein and the in vitro translated hnRNP-A1 protein were used in the GST-binding assay, ^{35}S-labeled hnRNP-A1 was detected (Fig. 1A, lane 1). This interaction was specific for N protein because no ^{35}S-labeled hnRNP-A1 was pulled down with GST alone (Fig. 1A, lane 2). The interaction was also specific for hnRNP-A1 because neither ^{35}S-labeled GFP (green fluorescence protein) nor HE (hemagglutinin/esterase), another MHV structural protein, was brought down by GST–N (Fig. 1A, lanes 3 and 4, respectively). Interestingly, when the in vitro translation products of hnRNP-A1 and HE were mixed, GST–N protein selectively brought down hnRNP-A1 but not HE (Fig. 1A, lane 5), indicating that the interaction between GST–N and hnRNP-A1 was specific. Similarly, when the N protein was translated in vitro and hnRNP-A1 was expressed as a GST–fusion protein, N protein specifically bound to the GST–A1 Sepharose beads, but did not bind to GST (Fig. 1B). These results demonstrate that N protein directly interacts with hnRNP-A1 in vitro.

Next, we employed co-immunoprecipitation as an alternative approach to determine the interaction between
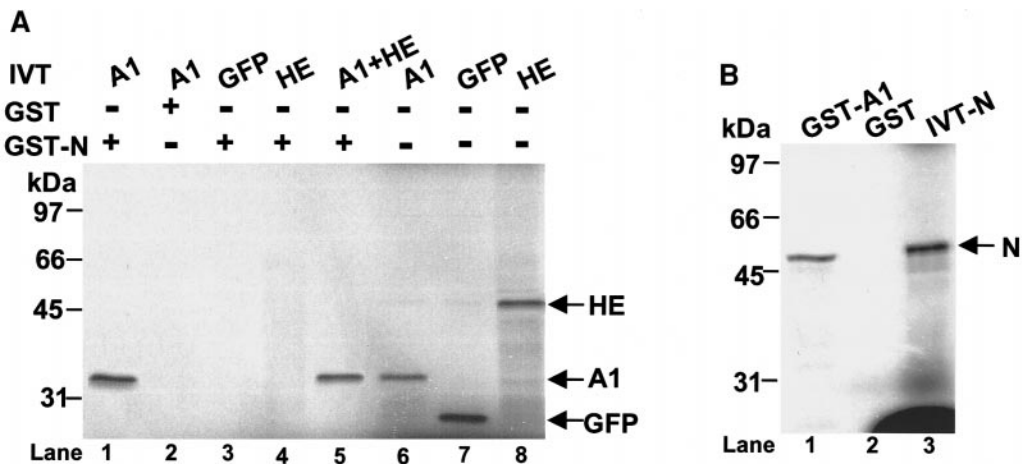
WANG AND ZHANG

FIG. 1. Interactions between MHV N protein and hnRNP-A1 *in vitro*. One of the two interacting proteins was expressed as a GST–fusion protein and the other was labeled with [^{35}S]methionine in an *in vitro* translation reaction (IVT). Protein–protein interactions between GST–fusion protein and *in vitro* translated protein were determined by a GST-binding assay (see Materials and Methods). (A) Components of the reaction in each lane are shown at the top left and are indicated either by names or by plus (presence) and minus (absence) signs at the top of the figure. A1, hnRNP-A1; HE, MHV hemagglutinin/esterase protein; GFP, green fluorescence protein. Lane 1, GST–N plus IVT-A1; lane 2, GST plus IVT-A1; lane 3, GST–N plus IVT-GFP; lane 4, GST–N plus IVT-HE; lane 5, GST–N plus IVT-A1 and IVT-HE. Lanes 6, 7, and 8 represent 10% of the input volume of *in vitro* translation products used for the binding reactions as protein controls. (B) Lane 1, GST-A1 plus IVT-N; lane 2, GST plus IVT-N; lane 3, IVT-N alone (10% of the input volume of IVT products used for the binding reaction). Protein complexes were analyzed by SDS–polyacrylamide gel electrophoresis (10% gel). The gel was autoradiographed. The *in vitro* translated products are indicated on the right and molecular mass markers in kilodalton on the left.

hnRNP-A1 and N proteins. GST–N fusion protein was eluted from the glutathione–Sepharose beads, mixed with the ^{35}S-labeled hnRNP-A1, and immunoprecipitated with an N-specific monoclonal antibody (MAb). The resultant complexes were isolated with protein A–agarose beads and separated by sodium dodecyl sulfate–polyacrylamide gel electrophoresis (SDS–PAGE). As expected, hnRNP-A1 was detected only when the GST–N fusion protein was present (Fig. 2, lane 5); no hnRNP-A1 was coprecipitated by the N-specific MAb when GST alone was used (Fig. 2, lane 6), again demonstrating that N protein specifically interacted with hnRNP-A1. The results also showed that the MAb interacted specifically with N protein (Fig. 2, lane 4) and did not cross-react with hnRNP-A1 protein (Fig. 2, lane 2).

Because it is known that both hnRNP-A1 and N proteins interact with viral RNAs and some other RNAs, it is possible that hnRNP-A1 might be brought down indirectly through its interaction with RNAs. To investigate this possibility, rabbit reticulocyte lysates were treated with micrococcal nuclease following the *in vitro* translation reaction. This treatment did not affect the interaction between hnRNP-A1 and N proteins (Fig. 3A), indicating that hnRNP-A1 directly interacted with N protein. The specificity of this interaction was further demonstrated by a competition assay using bovine serum albumin as a nonspecific competitor (Fig. 3B). A cold specific competitor (unlabeled hnRNP-A1) could not be used for this experiment due to the formation of oligomers with labeled hnRNP-A1 (data not shown). Oligomerizations among hnRNP-A1 proteins have been reported (Dreyfuss

et al., 1993). To further establish the specificity of this interaction, we used a modified protocol for the competition assay using purified GST–N(III) protein as a specific competitor. GST–N(III) contains the last domain of N protein, which interacts with hnRNP-A1 but which does not interact with itself (N protein) (Fig. 6). Various amounts (0–40 μg) of purified GST–N(III) protein were mixed with a fixed amount (2 μl) of *in vitro* translated hnRNP-A1 in a protein-binding buffer (the same for GST-binding assay) and the mixture was incubated at 4°C overnight. Before the GST-binding assay was performed, the GST-binding sites on GST–N-immobilized Sepharose beads were saturated with an excess amount of GST; without this treatment, GST–N(III)–hnRNP-A1 complexes would bind to unsaturated beads in the GST-binding reaction through interactions between GST and glutathione on the beads and not through interactions between hnRNP-A1 and the N moiety of GST–N protein. After saturation, the same amount of GST–N–Sepharose beads were used in a standard GST-binding assay by mixing it with GST–N(III)–^{35}S-hnRNP-A1. The complexes were then separated by SDS–PAGE. If the interaction between GST–N(III) and ^{35}S-hnRNP-A1 is specific, with increasing amounts of GST–N(III), decreasing amounts of free ^{35}S-hnRNP-A1 would be brought down by GST–N–Sepharose beads. As expected, ^{35}S-hnRNP-A1 was indeed competed by GST–N(III) protein in a concentration-dependent manner. A decrease of ^{35}S-hnRNP-A1 was readily detectable even when only 10 μg of the competitor GST–N(III), an equivalent amount to GST–N, was used in this assay (Fig. 3C, lane 3). When the
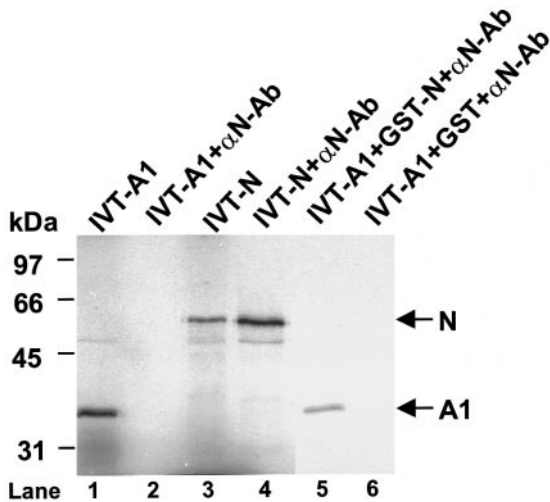
FIG. 2. Co-immunoprecipitation of *in vitro* translated hnRNP-A1 and GST-N proteins by an N-specific antibody. hnRNP-A1 was labeled with [^{35}S]methionine in an *in vitro* translation reaction (IVT-A1), and N protein was expressed as a GST–fusion protein (GST–N). Immunoprecipitation of IVT-A1 by the N-specific antibody (αN-Ab) was performed in the presence of GST–N fusion protein (lane 5) or GST protein (lane 6). The immunocomplex was isolated with protein A–agarose beads and was separated by SDS–polyacrylamide gel (10%) electrophoresis. The gel was autoradiographed. Lanes 1 and 3 represent 10% of the input volume of *in vitro* translation products of A1 (IVT-A1) and N (IVT-N), respectively, used for immunoprecipitation. Lane 2, IVT-A1 plus anti-N-Ab, and lane 4, IVT-N plus anti-N-Ab, were controls for the specificity of αN-Ab. Bands representing hnRNP-A1 and N are indicated by arrows on the right, molecular mass markers in kilodalton are on the left, and lane numbers are indicated at the bottom.

amount of GST–N(III) was increased twofold (20 μg), hnRNP-A1 was almost completely competed away (Fig. 3C, lane 4). No hnRNP-A1 could bind to GST–N Sepharose beads when 40 μg of the competitor GST–N(III) was used, which is a four times excess over GST–N (Fig. 3C, lane 5). Taken together, these results demonstrate that N protein has protein-binding properties and that it interacts specifically and directly with hnRNP-A1 *in vitro*.

Characterization of the protein-binding sites on the N protein

Based on a sequence analysis of the N genes of five MHV strains, Parker and Masters (1990) suggested that N protein is composed of three highly conserved structural domains connected to each other by two less conserved spacer sequences. The amino-terminal two domains (domains I and II) are basic and the carboxyl-terminal domain is acidic. Although the RNA-binding property of N protein has been mapped to be within the middle domain (domain II) (Masters, 1992; Nelson and Stohlman, 1993), the functions of domains I and III are unknown. Also, the protein-binding property and binding sites on the N protein have not been reported previously. To dissect the protein-binding site(s) of the N protein, we made a series of deletion constructs by PCR (Fig. 4A)

and cloned each into a pGEX4-1 vector for expression as GST–fusion proteins. All proteins were expressed in a substantial amount and the size of each fusion protein corresponded to its expected molecular weight (Fig. 4B). Although some degradation was observed in a few proteins, the full-length products were still predominant in these proteins (Fig. 4B, lanes 5, 8, 12, and 14). These truncated GST–N fusion proteins were then used in a GST-binding assay for determining their binding capacity with the *in vitro* translated, radiolabeled hnRNP-A1. As shown in Fig. 5A, hnRNP-A1 bound to all GST–fusion proteins containing domains I, IIA, and III, but did not bind to the second half of the middle domain [GST–N(IIB), lane 9]. Further deletions of domains I and II of the N protein did not significantly affect the binding with hnRNP-A1 (Fig. 5B). We thus conclude that N protein contains at least two protein-binding sites: one at the amino terminus from amino acids 1 to 292, and the other at the carboxyl terminus from amino acids 391 to 455 (Fig. 7). Because all N deletion constructs within the amino-terminal region (domains I and IIA) bound to hnRNP-A1 with similar affinities (Fig. 5B), we could not determine the exact number of binding sites on this domain (Fig. 7). The reason for this ambiguity is unknown. One possibility is that the amino-terminal-binding region contains multiple binding sites. Multiple binding sites in a protein are common among chaperone proteins with protein-interacting properties such as hnRNP-A1 (Cartegni *et al.,* 1996).

Since N protein has protein-binding properties as shown above, an interesting question is whether N protein can interact with itself. If so, what is the exact location of the protein-binding site? To address this question, we used GST–N and its deletion derivatives immobilized on Sepharose beads and the *in vitro* translated, ^{35}S-labeled full-length N protein in a GST-binding assay to determine their interactions. As shown in Fig. 6, the full-length N protein did indeed interact with itself (lane 3). Furthermore, it interacted with domains I and IIA (lanes 3 and 5) but did not bind to domains III and IIB (lanes 4 and 6). We conclude that N protein can interact with itself but that the binding site for N is located in domains I and IIA and not in domains IIB and III. Thus, the protein-binding sites on N protein for binding of N and hnRNP-A1 are different (Fig. 7).

N protein co-localizes with hnRNP-A1 in the cytoplasm of MHV-infected cells

Although cytoplasmic relocalization of hnRNP-A1 was previously observed in MHV-infected cells, it was not clear what the correlation between cytoplasmic relocalization of hnRNP-A1 and virus replication is, because only a single-labeling immunofluorescence assay was performed (Li *et al.,* 1997). This question is important because it may relate the biological role of hnRNP-A1 to

viral replication and transcription. Also, the above *in vitro* results suggest that hnRNP-A1 protein may interact with N protein *in vivo.* We addressed this issue in the present study by employing the double-staining immunofluorescence technique so that the localization of both hnRNP-A1 protein and the N protein (an indicator of virus gene expression) can be monitored simultaneously. Cells were infected with MHV-JHM virus at a multiplicity of infection (m.o.i.) of 1. At various times postinfection (p.i.), cells were stained simultaneously with two primary antibodies (a chicken antiserum specific to hnRNP-A1 and a mouse MAb specific to N protein) and two secondary antibodies (goat anti-chicken IgG conjugated with rhodamine and rabbit anti-mouse IgG conjugated with fluorescein, respectively). Mock-infected cells were used as a control. Results showed that hnRNP-A1 predominantly localized in the nucleus of mock-infected cells or of cells infected with MHV at 0 h p.i. (Fig. 8b). No N protein was detected in these cells at this time point (Fig. 8a). At 2 h p.i., cytoplasmic localization of hnRNP-A1 was occasionally observed, whereas the expression of the N protein was still undetectable (data not shown). At 5 h p.i., both N and hnRNP-A1 proteins were detectable and they appeared to colocalize in the cytoplasm under microscopic examination. Confocal laser scanning microscopy further confirmed their cytoplasmic colocalization (data not shown). At 7 h p.i., most cells were fused and syncytia were often observed. Cytoplasmic colocalization of the two proteins was more pronounced at this time point but the cytoplasmic staining generally became weaker, possibly due to diffusion of the dyes (Figs. 8d–8f). It is noted that the cytoplasmic localization of hnRNP-A1 was not found in all infected cells. In some of the infected cells, determined by the presence of N protein [fluorescein isothiocyanate (FITC)-staining], hnRNP-A1 remained in the nucleus (data not shown). Consistent with this observation is the finding that hnRNP-A1 remained in the nucleus of some cells within a syncytium (Fig. 8e). In contrast, N protein was detected in the cytoplasm of all cells within the syncytium (Fig. 8d). The detection of nuclear staining of hnRNP-A1 within the syncytia also suggests that these nuclear-stained cells were not infected primarily but were fused with neighboring infected cells (fusion from within). Importantly, hnRNP-A1 colocalized with N protein in the perinuclear region of the infected cells (Fig. 8f), where MHV replication and transcription complex also localizes (Denison *et*
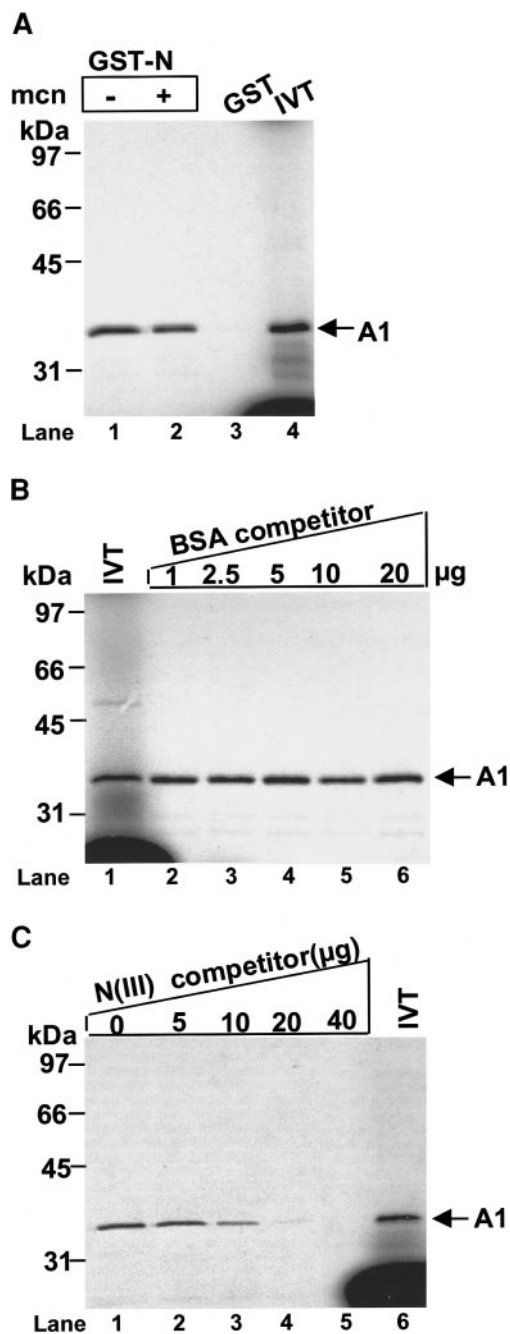
FIG. 3. The interaction between N protein and hnRNP-A1 is specific. The GST-binding assay (see Materials and Methods) was carried out to determine the interactions between GST–N and the *in vitro* translated (IVT) hnRNP-A1. (A) Lanes 1 and 2 indicate the interaction between IVT-A1 and GST–N following treatment of the lysates without (−) or with (+) micrococcal nuclease (mcn), respectively. Lane 3, GST plus IVT-A1 without micrococcal nuclease treatment; lane 4, 10% of the input volume of the *in vitro* translation products used for the binding reaction. The arrow indicates A1 protein. (B) Competition assay. Various amounts (μg) of bovine serum albumin (BSA) as a nonspecific protein competitor were added to the GST–N–Sepharose beads prior to the addition of IVT-A1 in a GST finding assay (lanes 2 to 6). Lane 1, 10% of the input volume of IVT products. The arrow indicates A1 protein. (C) Competition assay with a specific competitor. Various amounts (0–40 μg) of GST–N(III) fusion protein were added to a fixed amount of IVT-A1 (2 μl) in a protein binding buffer, and the reaction was incubated at 4°C

overnight (lanes 1 to 5). Then, the GST–N (full-length) protein immobilized on the Sepharose beads (10 μl), which were saturated by the addition of an excessive amount of GST, was mixed with IVT-A1 and GST–N(III) complex. Proteins not bound to the beads were washed away and bound proteins were analyzed by electrophoresis on a 10% polyacrylamide gel. Lane 6, 10% of the input volume of IVT-A1 products. The arrow indicates the A1 protein. Molecular mass markers in kDa are indicated on the left.
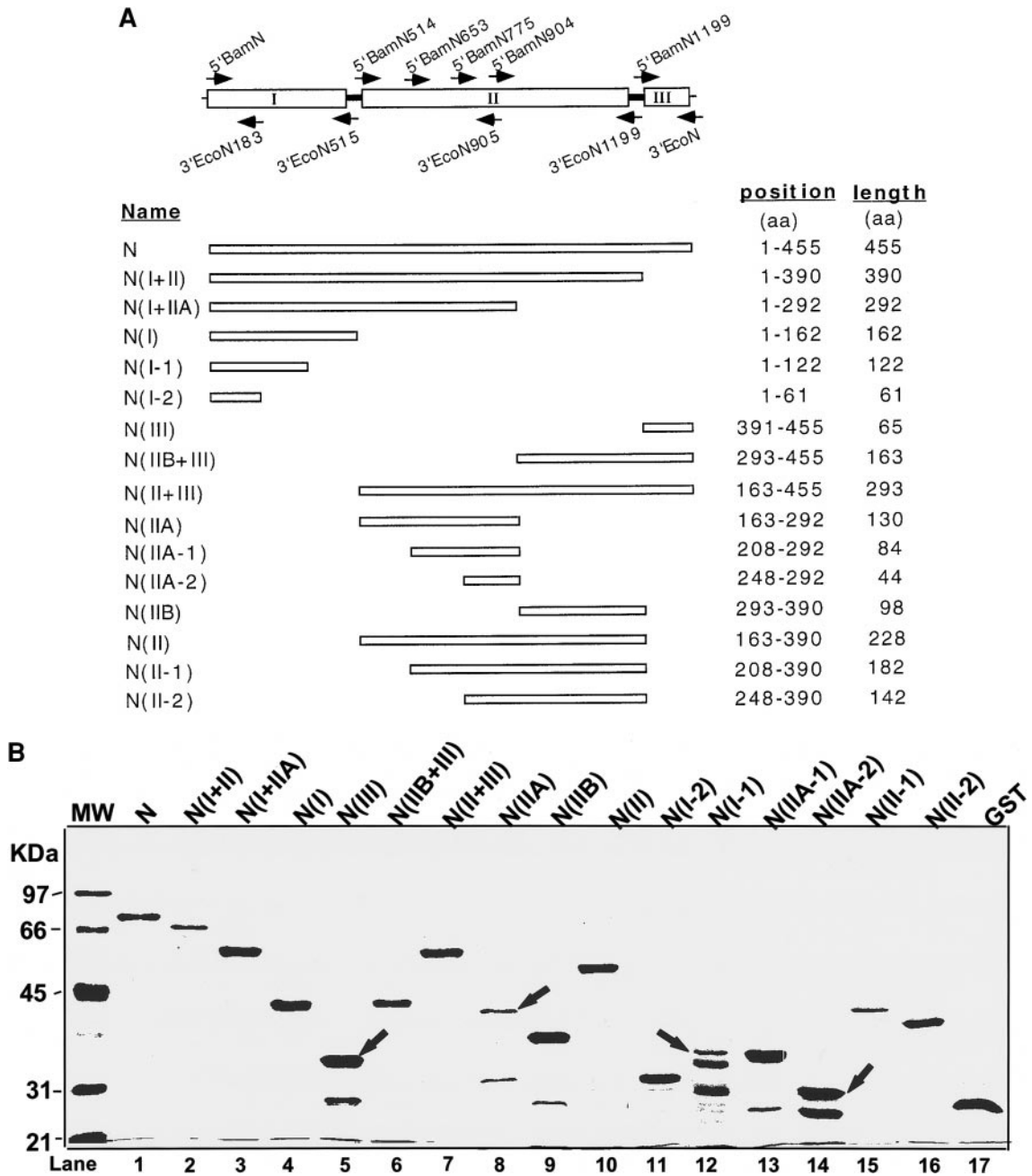
FIG. 4. Structural diagram of the N constructs and expression of GST–N fusion proteins. (A) The three structural domains (I, II, and III) of the N protein and all primers used for PCR amplification and construction are shown at the top. The assignment of the domains is based on the proposal of Parker and Masters (1990). Below is the diagram of the full-length and various deletion N constructs. The names of individual constructs are shown on the left, and their amino acid positions and lengths are shown on the right. (B) Coomassie brilliant blue staining of a protein gel showing the correct expression of GST–N fusion proteins (lanes 1 to 17). Arrows indicate the corresponding protein species. Names of individual GST–fusion proteins are indicated on the top and molecular mass markers in kDa on the left.

al., 1999; Shi et al., 1999). These results suggest a possible link between hnRNP-A1 and N proteins and MHV replication/transcription apparatus.

Interactions between N protein and hnRNP-A1 in MHV-infected cells

The above finding on colocalization of hnRNP-A1 and N proteins, however, did not indicate a physical interac-

tion between them. To demonstrate a specific interaction between the two proteins in virus-infected cells, we employed an immunoaffinity method. If hnRNP-A1 interacts with the N protein, immunoprecipitation of the cytoplasmic extracts from MHV-infected cells by an antibody specific to one of the two proteins would bring down the other interacting partner. Two opposing approaches were employed. In the first experiment, we used an
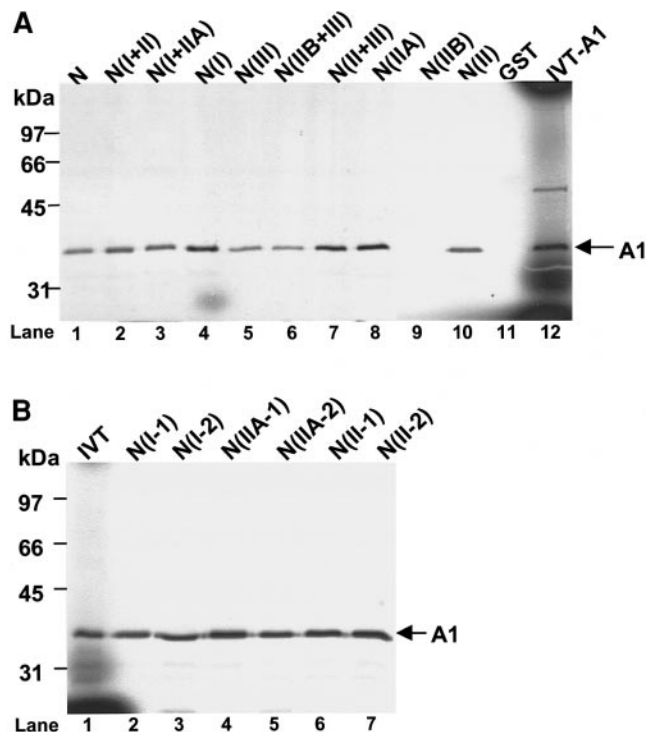
FIG. 5. Dissection of the hnRNP-A1-interacting domains of MHV N protein. The interactions between GST–N fusion proteins and *in vitro* translated hnRNP-A1 (IVT-A1) were determined in a GST-binding assay (see Materials and Methods). Proteins were analyzed by SDS–polyacrylamide gel (10%) electrophoresis. The gel was autoradiographed. The names of individual GST–N fusion proteins are indicated at the top of the figure and corresponding lanes on the bottom (lanes 1 to 11). Lane 12 in (A) and lane 1 in (B) represent 10% of the input volume of the IVT-A1 products used for the interaction. The arrow denotes hnRNP-A1. Molecular mass markers in kDa are shown on the left.

N-specific MAb to co-immunoprecipitate the N and any other possible interacting proteins in virus-infected cytoplasmic extracts. The immunocomplexes were separated by SDS–polyacrylamide gel electrophoresis and were transferred to nitrocellulose membrane. The presence of hnRNP-A1 was then detected by Western blot analysis with a MAb specific to hnRNP-A1 and a goat anti-mouse IgG antibody conjugated with peroxidase. Consistent with the results from the fluorescence-staining experiment, co-immunoprecipitation of hnRNP-A1 by the N antibody was detectable at 5 h p.i. and became more pronounced at 7 and 9 h p.i. (Fig. 9A), at which time points viral transcription also reaches a plateau. In the second experiment, we used the hnRNP-A1-specific MAb for immunoprecipitation and the N-specific MAb for Western blot analysis to detect whether N protein could be coprecipitated by the hnRNP-A1-specific MAb. And the results showed that this was indeed the case (Fig. 9B). These data indicate that N protein interacted directly with hnRNP-A1 in MHV-infected cells.

However, it is also possible that RNAs present in the infected cell lysates might have mediated this interaction as discussed above for *in vitro* experiments. To investi-

gate this possibility, cytoplasmic extracts were treated with micrococcal nuclease prior to immunoprecipitation. This treatment effectively removed the exogeneously added mRNAs in a control experiment (data not shown) but did not significantly affect the amount of hnRNP-A1 precipitated by the anti-N antibody in Western blot compared to that of the untreated extracts (Fig. 9C), indicating that viral and cellular mRNAs present in the lysates, if any, did not have a bridging effect on this interaction.

Interactions between N protein and hnRNP-A1 in yeast

Next, we employed the yeast two-hybrid system to further determine whether N protein interacts with hnRNP-A1 *in vivo*. The yeast two-hybrid system, developed by Fields and Song (1989), has been widely used as a powerful tool to screen a library for a gene encoding a novel protein that interacts with a known target protein or to test two known, previously cloned proteins for interaction *in vivo*. We cloned the full-length N gene and hnRNP-A1 gene fused either to the Gal4-DNA-binding domain (DBD) or to the Gal4-transcriptional activation domain (AD) of the vectors pAS2 (plasmid encoding the DBD) and pACT2 (plasmid encoding the AD), respectively. We then co-transformed the pair of plasmid DNAs (pAS2-N and pACT2-A1, or pAS2-A1 and pACT2-N) into the yeast strain Y187. Colonies grown on synthetic dropout (SD) agar plates containing a selection medium [a synthetic minimal medium lacking tryptophan and leucine (SD/-Trp/-Leu)] after incubation for 3 to 5 days at
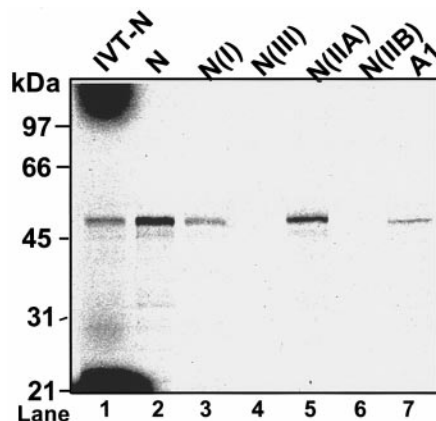

FIG. 6. MHV N protein interacts with itself *in vitro*. The interaction between GST–N fusion proteins and *in vitro* translated N protein (IVT-N) was determined in a GST binding assay (see Materials and Methods). Proteins were analyzed by SDS–polyacrylamide gel (10%) electrophoresis. The gel was autoradiographed. The names of individual GST–N fusion proteins are indicated at the top of the figure and corresponding lane numbers at the bottom (lanes 2 to 6). Lane 7 shows the interactions between IVT-N and GST–A1 as a positive control. Lane 1 represents 10% of the input volume of IVT-N products used for the reactions. Molecular mass markers in kDa are shown on the left. Note that the relative intensity of the bands does not indicate their binding affinities in this figure.
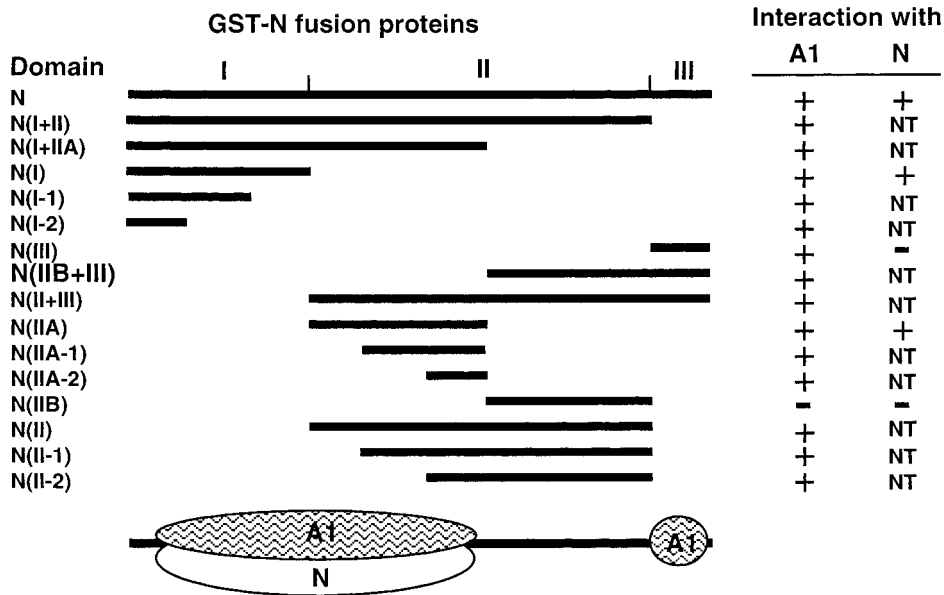
GST-N fusion proteins

Interaction with

Domain		A1	N
N		+	+
N(I+II)		+	NT
N(I+IIA)		+	NT
N(I)		+	+
N(I-1)		+	NT
N(I-2)		+	NT
N(III)		+	−
N(IIB+III)		+	NT
N(II+III)		+	NT
N(IIA)		+	+
N(IIA-1)		+	NT
N(IIA-2)		+	NT
N(IIB)		−	−
N(II)		+	NT
N(II-1)		+	NT
N(II-2)		+	NT

FIG. 7. Summary of interactions between hnRNP-A1 and N proteins and between N and N proteins. Schematic diagram of GST–N fusion proteins: only the N portions are shown and domains I–III are indicated. Interactions between various GST–N fusion proteins and the full-length *in vitro* translated hnRNP-A1 (A1) or N (N) proteins are indicated on the right. +, positive interaction; −, negative interaction; NT, not tested. The approximate binding sites for A1 and N on the N protein are shown at the bottom.

30°C were tested for the expression of β-galactosidase activity by a colony-lift filter assay. As shown in Table 1, co-transformation of pAS2-N and pACT2-A1 or of pAS2-A1 and pACT2-N resulted in the expression of β-galactosidase activity, indicating that the N protein interacted with hnRNP-A1 in yeast. In the control experiments, the same yeast strain, which was co-transformed with two empty vectors, did not express β-galactosidase; when the yeast was co-transformed with pLAM5′-1 and pTD1-1, which encodes an unrelated protein Gal4-DBD/human Lamin C hybrid and Gal4-AD/SV40 large T antigen, respectively, no β-galactosidase was detected. Yeast transformed with a single vector (either pAS2 or pACT2) did not grow in the selection medium, indicating that there were no nonspecific interactions between proteins expressed from the two vectors. Strong expression of β-galactosidase was detected in the yeast co-transformed with pVA3-1 (plasmid encoding Gal4-DBD/murine p53) and pTD1-1, which serves as a positive control. The yeast co-transformed with pAS2-A1 and pACT2-A1 grew in the selection medium and expressed β-galactosidase slightly more than that co-transformed with pAS2-A1 and pACT2-N or with pAS2-N and pACT2-A1, but significantly lower than the positive control (Table 1), indicating that hnRNP-A1 self-interaction appeared stronger than that between hnRNP-A1 and N protein. This result is also consistent with a previous report that showed that hnRNP-A1 self-interaction was approximately 30% of the interaction between p53 and SV40 large T antigen in the yeast two-hybrid system (Cartegni *et al.,* 1996).

DISCUSSION

In the present study, we employed a series of biochemical methods to test the hypothesis that MHV N protein interacts directly with a cellular protein hnRNP-A1, both of which have been implicated in the regulation of MHV RNA replication and transcription (Compton *et al.,* 1987; Stohlman *et al.,* 1988; Zhang and Lai, 1995; Li *et al.,* 1997). Our results clearly establish that N protein specifically interacts with hnRNP-A1 *in vitro,* in virus-infected cells, and in yeast. To our knowledge, this is the first report that coronavirus N protein has a protein-binding activity, binding to a cellular protein of the putative transcription and replication complex, in addition to its known RNA-binding activity.

Our results showed that N and hnRNP-A1 proteins colocalized in the cytoplasm of MHV-infected cells, thus extending our previous observation on intracellular redistribution of a single hnRNP-A1 protein (Li *et al.,* 1997). Significantly, we found that the two proteins co-localized predominantly in the perinuclear region of MHV-infected cells (Fig. 8f), where active MHV replication/transcription complexes reside (Shi *et al.,* 1999; Denison *et al.,* 1999). This suggests that both N and hnRNP-A1 proteins are possibly the components of the MHV replication/transcription complex and that their interaction may be involved in regulation of MHV RNA synthesis. The cytoplasmic redistribution of hnRNP-A1 in MHV-infected cells observed in this and a previous study (Li *et al.,* 1997) suggests a physical and, possibly, functional link between hnRNP-A1 and MHV infection. Alternatively, cyto-
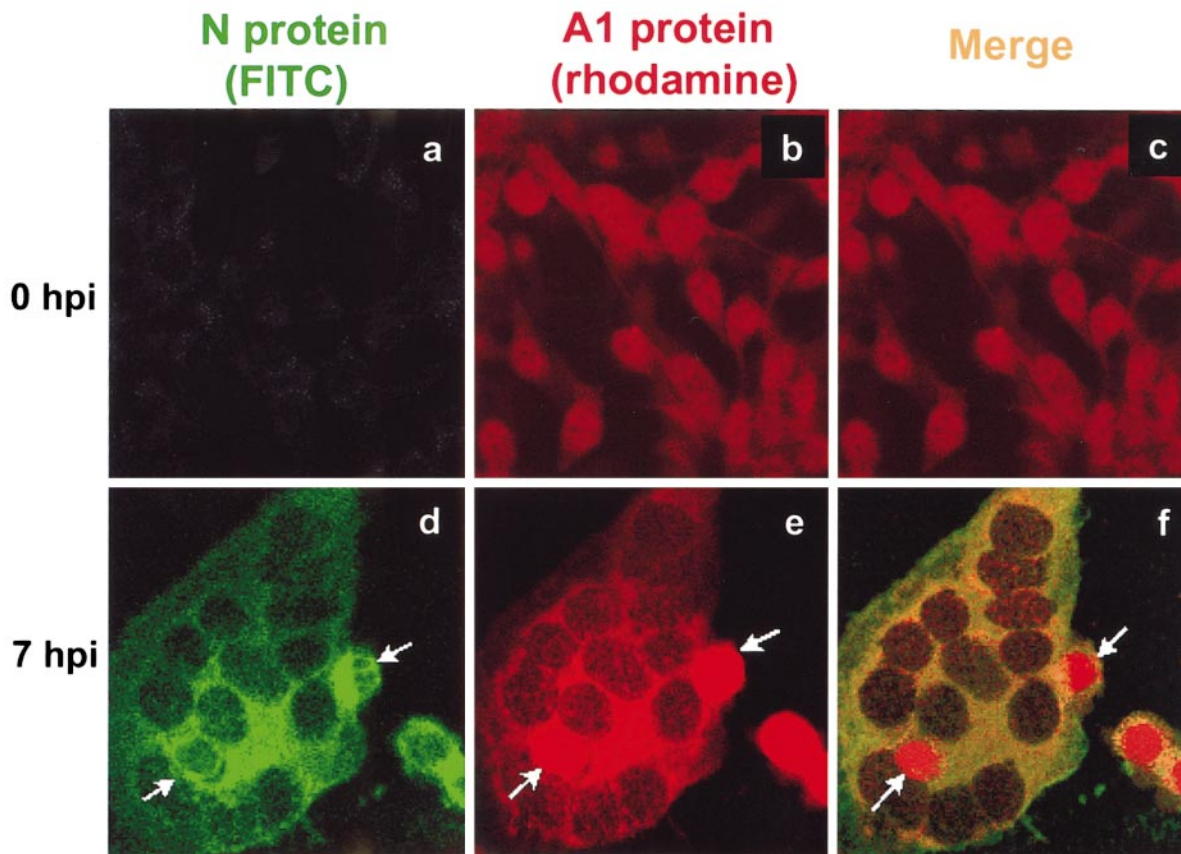
FIG. 8. Co-localization of MHV N protein and cellular hnRNP-A1 in the cytoplasm of MHV-infected cells. Cells were infected with MHV JHM strain at a multiplicity of infection of 1. At 0 (a–c) and 7 (d–f) hpi, cells were stained with an hnRNP-A1-specific chicken antiserum and a monoclonal antibody specific to N protein, followed by the rhodamine-conjugated anti-chicken IgG antibody and a FITC-conjugated anti-mouse IgG antibody. Stained cells were observed by laser confocal microscopy (Zeiss). (a and d) FITC-stained (green); (b and e) rhodamine-stained (red); (c and f) merged image (orange). Arrows in d to f indicate the nuclear localization of hnRNP-A1 (red) but cytoplasmic localization of the N protein (green) in these cells within a syncytium.

plasmic relocalization of hnRNP-A1 may be a passive diffusion process due to leakage of the nuclear membrane caused by MHV infection. This is less likely, however, because another nuclear protein, Sam68, which relocalizes from the nucleus to the cytoplasm in poliovirus-infected cells (McBride et al., 1996), remains in the nucleus of MHV-infected cells (Li et al., 1997). Also, the observation that hnRNP-A1 remained in the nuclei of many MHV-infected cells, which exhibited positive fluorescence staining of N protein (data not shown), argues that MHV infection does not cause leakage of the nuclear membrane. In no instance we were able to detect cytoplasmic localization of hnRNP-A1 in noninfected cells even though hnRNP-A1 shuttles constantly between the nucleus and the cytoplasm.

The interaction between N and hnRNP-A1 might provide one of the mechanisms by which MHV regulates its discontinuous transcription. We previously proposed that the interaction between the leader and the intergenic sequence of the template RNA, which is a critical step in the initiation of mRNA transcription (based on the leader-primed transcription model), is mediated through protein–RNA and protein–protein interactions, i.e., cellular

and/or viral proteins first bind to the leader and the intergenic sequence of the template RNA through protein–RNA interactions; these two discontiguous RNA sequences are then brought together to form a transcription initiation complex through protein–protein interactions (Zhang and Lai, 1995). It has been shown that hnRNP-A1 binds to the intergenic sequence of the negative-strand template RNA (Zhang and Lai, 1995) and that the N protein binds to the leader RNA (Baric et al., 1988; Stohlman et al., 1988). Thus, an attractive possibility is that the interaction between hnRNP-A1 and N proteins would bring the leader RNA to the intergenic sequence of the template to form a ribonucleoprotein complex, which then regulates mRNA transcription. Alternatively, the interaction between N and hnRNP-A1 might also mediate discontinuous transcription during negative-strand synthesis. In that case, N protein would bind to the leader RNA of the genomic RNA template; hnRNP-A1 protein would bind to the intergenic region of the nacent minus-strand RNA transcript. hnRNP-A1 might be already present in the transcription complex or recruited to the intergenic site once the transcription complex moves toward the intergenic region. The presence of hnRNP-A1
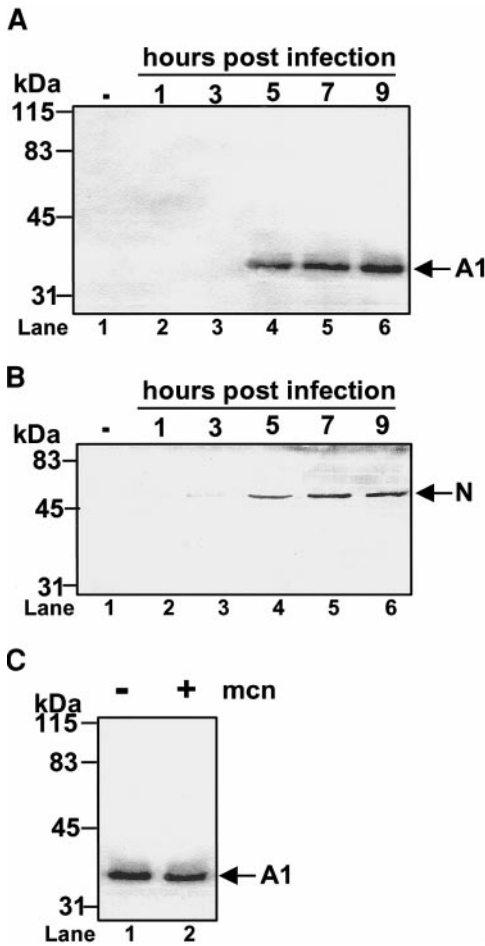
FIG. 9. Co-immunoprecipitation of hnRNP-A1 and N proteins from the cytoplasmic extracts of MHV-infected cells by an antibody specific to N or hnRNP-A1. (A) Cells were uninfected (−) (lane 1) or infected with MHV JHM strain at a multiplicity of infection of 1 (lanes 2 to 6). At 1, 3, 5, 7, and 9 h postinfection (lanes 2 to 6), cytoplasmic lysates were extracted and immunoprecipitated with an N-specific monoclonal antibody and protein A–agarose beads, and the immunocomplex was separated by electrophoresis on SDS–polyacrylamide gel (10%). Proteins were transferred to a nitrocellulose membrane and visualized by Western blot analysis using a monoclonal antibody specific to hnRNP-A1 and a peroxidase-conjugated secondary antibody against mouse IgG. The arrow indicates hnRNP-A1 detected in the Western blot. Molecular mass marker (M) in kilodalton (kDa) shown on the left. (B) Experiments were performed essentially the same as described in (A), except that a monoclonal antibody specific to hnRNP-A1 was used for immunoprecipitation and an N-specific monoclonal antibody for Western blot analysis. The arrow indicates the N protein detected in Western blot. (C) Effects of microccocal nuclease treatment. Experiments were done in a manner similar to that for (A) lane 6, except that the lysates were treated with (+) (lane 2) or without (−) (lane 1) micrococcal nuclease (mcn) prior to immunoprecipitation.

at the intergenic site may facilitate an efficient termination (pause) of transcription and resume transcription at the 3′-end of the leader through interaction with N and other RNA-binding proteins that are bound to the template leader region. Regardless of which model may be operative, our results are compatible with both models.

Recently, it has been shown that another cellular pro-

tein, polypyrimidine tract-binding protein (PTB or hnRNP I), binds to the leader RNA (Li *et al.,* 1999). Interaction between PTB and hnRNP-A1 has been documented (Dreyfuss *et al.,* 1993). It is thus conceivable that PTB and N protein may have a synergistic function in bringing the leader to the intergenic sequence for mRNA initiation through interactions with hnRNP-A1 (leader-primed transcription model) or in bringing the template leader to the intergenic site of minus-strand transcripts to resume transcription of the minus-strand subgenomic RNA (discontinuous transcription during minus-strand synthesis). Based on the observation that antibodies specific to N protein inhibited MHV RNA replication in an *in vitro* replication system, Compton *et al.* (1987) suggested that an interaction between the N protein and components of the replicase/transcriptase complex might be required for MHV RNA synthesis and that the binding of antibodies to N protein may inhibit such an interaction, thereby inhibiting viral RNA synthesis. Our findings on the interaction between N and hnRNP-A1 protein are consistent with this interpretation. It will be interesting to determine whether N protein also interacts with PTB or other protein components of the replicase complex.

Our *in vitro* data also establish that the N protein interacts with itself (Fig. 6). Does the N protein also interact with itself in virus-infected cells or in virions? We speculate that it probably does so. Robbins *et al.* (1986) detected both monomeric and multimeric N proteins in virions and infected cells. This suggests that N–N interactions may be important for encapsidation and virion

TABLE 1

Interaction between N and hnRNP-A1 in a Yeast Two-Hybrid System

DBD vectors[a]	AD vectors[a]	Protein interaction[b]
pVA3-1	pTD1-1	++++
pAS2	—	−
—	pACT2	−
pAS2	pACT2	−
pAS2-N	pACT2-A1	+
pAS2-A1	pACT2-N	+
pAS2-A1	pACT2-A1	++
pLAM5′-1	pTD1-1	−

[a] pAS2 and pACT2 are plasmid vectors encoding the Gal4 DNA-binding domain and transcriptional activation domain, respectively. pAS2-N, pAS2-A1, pACT2-N, and pACT2-A1 are plasmids containing the N and hnRNP-A1 fused either to DBD or AD, respectively. pVA3-1 and pTD1-1 are DBD- and AD–fusion plasmids encoding murine p53 and SV40 large T antigen, respectively, that provide a positive control for interacting proteins. pLAM5′-1 encodes a Gal4 DBD/human Lamin C hybrid and provides a control for fortuitous interaction between an unrelated DBD hybrid protein and an AD fusion protein.

[b] Protein interaction was determined by the colony-lift filter assay. −, white or no colony, indicates no interaction; +, blue colony, denotes a positive interaction. The larger the number of the plus signs, the darker the blue colony and the stronger the interaction.

TABLE 2

Oligonucleotides Used in PCR

Primer[a]	Sequence	Positions (nt)[b]
5'BamN	5'-TAG GGA TCC ATG TCT TTT GTT CCT-3'	30–44
5'BamN514	5'-TAG GGA TCC GAT ATT GTT GAA-3'	514–527
5'BamN653	5'-TAG GGA TCC CGT GGG CCA A-3'	653–666
5'BamN775	5'-TAG GGA TCC GGC CAG CCT AAG-3'	775–788
5'BamN904	5'-TAG GGA TCC AAT CAG AAT TTT G-3'	904–918
5'BamN1199	5'-TAG GGA TCC CCT AAG CCT CAG A-3'	1199–1212
3'EcoN183	5'-TAG GAA TTC TGC TTG GGC TGA-3'	183–170
3'EcoN515	5'-TAG GAA TTC GGC AGA GGT CCT AG-3'	515–502
3'EcoN905	5'-TAG GAA TTC GGG GCC TCT CTT TC-3'	905–892
3'EcoN1199	5'-TAG GAA TTC GCT CAC TAC ATC TG-3'	1199–1186
3'EcoN	5'-TAG GAA TTC TTA CAC ATT AGA GT-3'	1397–1384

[a] All 5'-primers are sense primers that contain a *Bam*HI site, while all 3'-primers are antisense primers that contain an *Eco*RI site.

[b] Nucleotide position 30 is the first nucleotide of the N gene open reading frame.

assembly. Identification of the interaction between N proteins in this study thus provides biochemical evidence in support of their finding (Robbins *et al.,* 1986). However, an intriguing question raised from our results is how the N–N protein interactions and the N-viral RNA interactions cooperate if the two different interaction processes are important for encapsidation, since both the protein-interacting (this study) and RNA-binding domains (Masters, 1992; Nelson and Stohlman, 1993) reside in a similar location of the N protein (domain IIA) (Figs. 5, 6, and 7). Does the protein–protein interaction interfere with the protein–RNA interaction during virus assembly or vice versa? An alternative explanation is that there are multiple protein-binding sites within domains I and IIA of the N protein. This region (approximately 300 amino acids) is large enough to accommodate both protein and RNA molecules at the same time. This is possible since N–N interactions occur independently in domains I and IIA (Fig. 6). Clearly, the biological role of the protein–protein interaction between N proteins in virus assembly requires further investigation.

MATERIALS AND METHODS

Virus, cells, and antibodies

The MHV JHM(2) strain (Makino and Lai, 1989) was used exclusively throughout this study. The murine astrocytoma cell line DBT (Hirano *et al.,* 1974) was used for virus growth, infection, and cell lysate preparation. The mouse MAb J3.3.1 specific to the carboxy-terminal of the MHV N protein (Flemming *et al.,* 1983) and the polyclonal chicken antiserum against an *Escherichia coli*-expressed murine hnRNP-A1 were kindly provided by Drs. Stephen Stohlman and Michael Lai (University of Southern California, Los Angeles), respectively. The specificity of the latter has been confirmed in Western blot analysis using murine hnRNP-A1 as antigens. A monoclonal antibody specific to the glycine-rich domain of hnRNP-A1

was kindly provided by Dr. Gideon Dreyfuss (University of Pennsylvania).

Plasmid constructions

To express the N protein and its deletion derivatives, a cDNA representing the N gene of MHV JHM strain was cloned into the vector pBluescript (Promega). Total RNAs were isolated from JHM virus-infected DBT cells by the Nonidet-P-40 (NP-40) method as described previously (Zhang *et al.,* 1994b). cDNAs were synthesized by reverse transcription using the primer 3'EcoN and amplified by PCR using a primer pair 5'BamN–3'EcoN (Table 2). PCR was performed at 95°C for 30 s, 56°C for 1 min, and 72°C for 2 min in a reaction buffer (20 mM Tris, pH 8.3, 25 mM KCl, 1.5 mM MgCl$_2$, 0.1% Tween 20, a 200 μM concentration of each NTP, 20 pmol of each primer) for 25 cycles. The same PCR conditions were used for all plasmid DNA constructions. The PCR fragments were digested with *Bam*HI and *Eco*RI and directionally cloned into pBluescript vector, generating pBS-N. Sequence of the clone was confirmed using a dye terminator kit (ABI) with the automatic DNA sequencer (Prizm Model 377, ABI) (Skinner and Siddell, 1983). pBS-N was then used for PCR amplication using various pairs of primers (see Table 2 and Fig. 4A). Because all sense primers contain a *Bam*HI site and all antisense primers an *Eco*RI site, the PCR fragments were digested with *Bam*HI and *Eco*RI and were directionally cloned into pGEX4-1, resulting in plasmids containing N and various domains of the N protein fused to the carboxyl-terminus of GST (Table 2 and Fig. 6A). All deletion constructs contain a stop codon at the 3'-end to ensure that no additional sequence of the vector would be expressed. For construction of pGST-NI-1, pGST-NI DNA was digested with *Dra*I and *Eco*RI, blunt-ended with T4 DNA polymerase, and self-ligated, such that the smaller *Dra*I–*Eco*RI fragment is deleted.

The previously constructed pBS-mA1 (Zhang *et al.,* 1999), which contains the full-length murine hnRNP-A1

sequence under the control of T7 promoter in pBluescript vector (Promega), was used for *in vitro* transcription and translation (see below). pGST-mA1 (Li *et al.,* 1997) was used for expressing hnRNP-A1 as a GST–fusion protein.

For control experiments, the previously constructed p25HE (Liao *et al.,* 1995) and pDE-GFP (Zhang, unpublished results) were used. p25HE and pDE-GFP are DI vectors expressing MHV hemagglutinin/esterase and the green fluorescence protein, respectively. Both DIs were digested with *Sna*BI and *Spe*I, blunt-ended with T4 DNA polymerase, and separated by agarose gel electrophoresis. The large fragments were self-ligated such that the HE or GFP ORF is under the control of T7 promoter.

For studying protein–protein interactions in the yeast two-hybrid system (Clontech), the Gal4-DNA-binding domain vector pAS2 was digested with *Xma*I and blunt-ended with T4 DNA polymerase. The N and hnRNP-A1 genes were isolated from the plasmids pBS-N and pGST-mA1, respectively, after digestion with *Bam*HI and *Eco*RI, blunt-ended with T4 DNA polymerase, and cloned into the blunt-ended pAS2 vector, resulting in pAS2-N and pAS2-A1, respectively. The orientation of the inserts was confirmed by restriction enzyme digestions. For construction of the Gal4–AD fusion vector, pACT2 was digested with *Sfi*I, blunt-ended with T4 DNA polymerase, and then digested with *Eco*RI. For preparing the N and hnRNP-A1 DNA fragments, pBS-N and pGST-mA1 were digested with *Bam*HI, blunt-ended, and then digested with *Eco*RI. The N and hnRNP-A1 genes were directionally cloned into pACT2 vector, generating pACT2-N and pACT2-A1, respectively.

In vitro transcription

For synthesis of RNAs used for *in vitro* translation, pBS-mA1 and pBS-N DNAs were linearized with *Eco*RI and subjected to *in vitro* transcription. The *in vitro* transcription was carried out in a standard (50 μl) transcription reaction containing 10 mM DTT, 1 U/μl RNasin, 0.5 mM each of ATP, CTP, UTP, and cap analog, and 0.05 mM GTP, 5 μg pBS-mA1 or pBS-N, 40 U T7 RNA polymerase at 37°C for 1 h according to the procedure recommended by the manufacturer (Promega). To remove the DNA template following the transcription reaction, RQ DNase (Promega) was added to a concentration of 1 unit/μg DNA and incubated at 37°C for 15 min. RNAs were purified by passing through a G25 or G50 column (5′ Primer 3′ Primer Inc.).

In vitro translation

The *in vitro* translation reaction was carried out in the rabbit reticulocyte lysate system in the presence of [^{35}S]methionine using the *in vitro* transcribed RNAs according to the manufacturer's recommendations (Promega). For some experiments, the lysate was treated with micrococcal nuclease (20 units/ml) in the presence of 1 mM calcium

chloride at 20°C for 10 min following the *in vitro* translation. The micrococcal nuclease was then inactivated by adding ethylene glycol-bis[*b*-aminoethyl ether]-*N,N,N′,N′*-tetraacetic acid at a final concentration of 2 mM.

Expression of GST–fusion proteins

The procedure for expressing GST–fusion proteins was based on the protocols as described (Smith and Johnson, 1988; Ausubel *et al.,* 1989). Briefly, pGST-mA1 and pGST-N and its deletion derivatives were transformed into *E. coli* (DH5α), and the transformants were grown at 37°C overnight in LB medium in the presence of ampicillin (100 μg/ml). Bacterial cultures were diluted with fresh LB medium and incubated for 4 h. At 2 h following the addition of isopropyl-thio-β-D-galactopyranoside, bacterial cultures were collected by centrifugation, resuspended in phosphate-buffered saline (PBS), and lysed by ultrasonication. Soluble proteins were purified with glutathione–Sepharose beads (Pharmacia). Bound proteins were then eluted by adding free glutathione at 10 mM in Tris buffer (pH 8.0).

Protein-binding assay

GST-binding assays were performed as previously described (Ausubel *et al.,* 1989). Briefly, 20 μl (approximately 10 μg) of GST–fusion proteins, coupled to Sepharose beads as described above, was mixed with 5 μl of *in vitro* translated ^{35}S-labeled A1 protein in 400 μl of binding buffer [40 mM (HEPES), pH 7.9, 100 mM KCl, 0.1% NP-40, 20 mM β-mercaptoethanol]. After a 4-h incubation at 4°C on a rotating platform, beads were pelleted by centrifugation at 1000 *g* in microcentrifuge tubes. The beads were then washed four times with 1 ml of the binding buffer. After the final wash, the bead pellets were resuspended in 20 μl of 1× Lammeli's sample buffer, boiled for 3 min, and recentrifuged, and the supernatants were analyzed by SDS–PAGE.

Immunofluorescence assay

DBT cells were grown on 8-well chamber slides (Lab Tak, Nunc, Nalgene) to subconfluency and infected with JHM virus at an m.o.i. of 1. At different times p.i., cells were fixed with 2% formaldehyde in PBS for 30 min at room temperature and permeabilized with acetone for 10 min at −20°C. Fixed cells were incubated at 37°C for 1 h in a humidified box following the addition of a mixture of two antibodies (mouse MAb J3.3.1 to N protein and a chicken antiserum to hnRNP-A1). After extensive washing with PBS, cells were stained simultaneously with two secondary antibodies [a rabbit anti-mouse IgG(H+L) antibody conjugated with FITC (Sigma) and a goat anti-chicken IgG(H+L) antibody conjugated with rhodamine (Sigma)] for 1 h at 37°C. Slides were then washed with PBS and mounted with coverslips. Intracellular localization of hnRNP-A1 and the N protein was observed under

the fluorescence microscope (Olympic 1000) with a wavelength of 254 nm for fluorescein and 355 nm for rhodamine. Photographs were taken using the confocal laser scanning microscope at the Core Facility of the Arkansas Cancer Research Center.

Extraction of cytoplasmic proteins

Extraction of cytoplasmic proteins was carried out as described previously (Zhang *et al.,* 1994b). Briefly, DBT cells were grown on 100-mm petri dishes to confluency and mock-infected or infected with JHM virus at an m.o.i. of 5. At various time points p.i., culture medium was removed. Cells were washed with ice-cold PBS twice, scraped with a rubber policeman into microcentrifuge tubes, and pelleted by centrifugation for 20 s. Cell pellets were resuspended in 300 μl of an extraction buffer [10 mM HEPES, pH 7.9, 10 mM KCl, 0.1 mM ethylenediami-netetraacetic acid, 1 mM dithiothreitol (DTT), 0.5 mM phenylmethylsulfonyl fluoride (PMSF)] by gentle pipetting and incubated on ice for 15 min. Following the addition of 25 μl of 10% NP-40, the cell suspension was mixed vigorously by vortexing for 20 s and centrifuged at 4°C for 2 min in a microcentrifuge. Pellets, which contain the nuclei, were discarded, and supernatants, which represent the cytoplasmic fraction, were collected. The protein concentration of the cytoplasmic extracts was determined with a Bio-Rad protein assay kit (Bio-Rad).

Immunoprecipitation

Immunoprecipitation was carried out in 500 μl of RIPA buffer (50 mM Tris, pH 7.4, 150 mM NaCl, 0.5% NP-40, 0.1% SDS, 1 mM PMSF) containing various amounts of infected and noninfected cytoplasmic extracts and the N-specific MAb J3.3.1 by constant rocking on a rocking platform at 4°C overnight. The antibody–antigen complexes were then precipitated with protein A–agarose beads at 4°C for 2–4 h. Agarose beads were washed three times with RIPA buffer. Proteins complexes were denatured by boiling for 3 min in Lammeli's sample loading buffer (100 mM Tris, pH 6.8, 200 mM DTT, 4% SDS, 0.2% bromophenol blue, 20% glycerol) and analyzed by PAGE. Proteins were then detected by Western blot analysis. For detection of *in vitro* protein–protein interactions, the GST–fusion proteins and the *in vitro*-translated proteins were mixed in RIPA buffer followed by the addition of N-specific MAb J3.3.1. Immunoprecipitates were analyzed by SDS–PAGE and the gels were exposed to X-ray film and autoradiographed.

Western blot

Western blot was performed as described previously (Zhang *et al.,* 1994a) with slight modifications. Briefly, following SDS–PAGE, proteins were transferred onto nitrocellulose membranes (Amersham) using a Bio-Rad Mini Transfer Blot at 60 V overnight at 4°C. Membranes were dried and blocked with either 10% skim milk or 2% bovine serum albumin in PBS for 2 h at 37°C. The membranes were incubated with the primary antibody (MAb specific to hnRNP-A1, 1:500 dilution) for 2 h at 37°C. After extensive washing, the membranes were incubated with a goat anti-mouse IgG secondary antibody conjugated with horseradish peroxidase (1:10,000 dilution) (Sigma) for 2 h. The substrate, diaminobenzidine (0.075%), and hydrogen peroxide (0.003%) were used to visualize the protein bands.

The yeast two-hybrid system

The Matchmaker Two-Hybrid System 2 (Clontech, Palo Alto, CA) was used for testing the interaction between the N protein and hnRNP-A1 *in vivo.* All procedures for growing yeast, transformation, selection, and β-galacto-sidase colony-lift filter assay essentially followed the protocol provided by the manufacturer (Clontech).

REFERENCES

Ausubel, F. M., Brent, R., Kingston, R. E., Moore, D. D., Seidman, J. G., Smith, J. A., and Struhl, K. (1989). *"Current Protocols in Molecular Biology."* Wiley, New York.

Baric, R. S., Nelson, G. W., Fleming, J. O., Deans, R. J., Keck, J. G., Casteel, N., and Stohlman, S. A. (1988). Interactions between coronavirus nucleocapsid protein and viral RNAs: Implications for viral transcription. *J. Virol.* **62,** 4280–4287.

Baric, R. S., Stohlman, S. A., Razavi, M. K., and Lai, M. M. C. (1985). Characterization of leader-related small RNAs in coronavirus-infected cells: Further evidence for leader-primed mechanism of transcription. *Virus Res.* **3,** 19–33.

Budzilowicz, C. J., Wilczynski, S. P., and Weiss, S. R. (1985). Three intergenic regions of coronavirus mouse hepatitis virus strain A59 genome RNA contain a common nucleotide sequence that is homologous to the 3′-end of the viral mRNA leader sequence. *J. Virol.* **53,** 834–840.

Cartegni, L., Maconi, M., Morandi, E., Cobianchi, F., Riva, S., and Biamonti, G. (1996). hnRNP-A1 selectively interacts through its Gly-rich domain with different RNA-binding proteins. *J. Mol. Biol.* **259,** 337–348.

Compton, S. R., Rogers, D. B., Holmes, K. V., Fertsch, D., Remenick, J., and McGowan, J. J. (1987). In vitro replication of mouse hepatitis virus strain A59. *J. Virol.* **61,** 1814–1820.

Denison, M. R., Spaan, W. J. M., van der Meer, Y., Gibson, C. A., Sims, A. C., Prentice, E., and Lu, X. T. (1999). The putative helicase of the coronavirus mouse hepatitis virus is processed from the replicase gene polyprotein and localizes in complexes that are active in viral RNA synthesis. *J. Virol.* **73,** 6862–6871.

Dreyfuss, G., Matunis, M. J., Pinol-Roma, S., and Burd, C. G. (1993).

hnRNP proteins and the biogenesis of mRNA. *Annu. Rev. Biochem.* **62,** 289–321.

Fields, S., and Song, O. (1989). A novel genetic system to detect protein-protein interactions. *Nature* **340,** 245–247.

Fisher, F., Stegen, C. F., Koetzner, C. A., and Masters, P. S. (1997). Analysis of a recombinant mouse hepatitis virus expressing a foreign gene reveals a novel aspect of coronavirus transcription. *J. Virol.* **71,** 5148–5160.

Flemming, J. O., Stohlman, S. A., Harmon, R. C., Lai, M. M. C., Frelinger, J. A., and Weiner, L. P. (1983). Antigenic relationships of murine coronaviruses: Analysis using monoclonal antibodies to JHM(MHV-4) virus. *Virology* **131,** 296–307.

Furuya, T., and Lai, M. M. C. (1993). Three different cellular proteins bind to the complementary sites on the 5′-end positive- and 3′-end negative-strands of mouse hepatitis virus RNA. *J. Virol.* **67,** 7215–7222.

Hirano, N., Fujiwara, K., Hino, S., and Matsumoto, M. (1974). Replication and plaque formation of mouse hepatitis virus (MHV-2) in mouse cell line DBT culture. *Arch. Gesamte Virusforsch.* **44,** 298–302.

Lai, M. M. C. (1998). Cellular factors in the transcription and replication of viral RNA genomes: A parallel to DNA-dependent RNA transcription. *Virology* **244,** 1–12.

Lai, M. M. C., Baric, R. S., Brayton, P. R., and Stohlman, S. A. (1984). Characterization of leader RNA sequences on the virion and mRNAs of mouse hepatitis virus-a cytoplasmic RNA virus. *Proc. Natl. Acad. Sci. USA* **81,** 3626–3630.

Lai, M. M. C., and Cavanagh, D. (1997). The molecular biology of coronaviruses. *Adv. Virus Res.* **48,** 1–100.

Lai, M. M. C., Patton, C. D., Baric, R. S., and Stohlman, S. A. (1983). The presence of leader sequences in the mRNA of mouse hepatitis virus. *J. Virol.* **46,** 1027–1033.

Lee, H. J., Shieh, C. K., Gorbalenya, A. E., Koonin, E. V., La Monica, N., Tuler, J., Bagdzyahdzhyan, A., and Lai, M. M. C. (1991). The complete sequence (22 kilobases) of murine coronavirus gene 1 encoding the putative proteases and RNA polymerase. *Virology* **180,** 567–582.

Li, H.-P., Zhang, X. M., Duncan, R., Comai, L., and Lai, M. M. C. (1997). Heterogeneous nuclear ribonucleoprotein A1 binds to the transcription-regulatory region of mouse hepatitis virus RNA. *Proc. Natl. Acad. Sci. USA* **94,** 9544–9549.

Li, H.-P., Huang, P., Park, S., and Lai, M. M. C. (1999). Polypyrimidine tract-binding protein binds to the leader RNA of mouse hepatitis virus and serves as a regulator of viral transcription. *J. Virol.* **73,** 772–777.

Liao, C.-L., Zhang, X. M., and Lai, M. M. C. (1995). Coronavirus defective-interfering RNA as an expression vector: The generation of a pseudorecombinant mouse hepatitis virus expressing hemagglutinin-esterase. *Virology* **208,** 319–327.

Makino, S., and Lai, M. M. C. (1989). Evolution of the 5′-end of genomic RNA of murine coronaviruses during passages in vitro. *Virology* **169,** 227–232.

Masters, P. S. (1992). Localization of an RNA-binding domain in the nucleocapsid protein of the coronavirus mouse hepatitis virus. *Arch. Virol.* **125,** 141–160.

McBride, A. E., Schlegel, A., and Kirkegaard, K. (1996). Human protein Sam68 relocalization and interaction with poliovirus RNA polymerase in infected cells. *Proc. Natl. Acad. Sci. USA* **93,** 2296–2301.

Nelson, G. W., and Stohlman, S. A. (1993). Localization of the RNA-binding domain of MHV nucleocapsid protein. *J. Gen. Virol.* **74,** 1975–1979.

Pachuk, C. J., Bredenbeek, P. J., Zoltick, P. W., Spaan, W. J. M., and Weiss, S. R. (1989). Molecular cloning of the gene encoding the putative polymerase of mouse hepatitis coronavirus strain A59. *Virology* **171,** 141–148.

Parker, M. M., and Masters, P. S. (1990). Sequence comparison of the N genes of five strains of the coronavirus mouse hepatitis virus

suggests a three domain structure for the nucleocapsid protein. *Virology* **179,** 463–468.

Peng, D., Koetzner, C. A., McMahon, T., Zhu, Y., and Masters, P. S. (1995). Construction of murine coronavirus mutants containing interspecies chimeric nucleocapsid proteins. *J. Virol.* **69,** 5475–5484.

Robbins, S. G., Frana, M. F., McGowan, J. J., Boyle, J. F., and Holmes, K. V. (1986). RNA-binding proteins of coronavirus MHV: Detection of monomeric and multimeric N protein with an RNA overlay-protein blot assay. *Virology* **150,** 402–410.

Sawicki, S. G., and Sawicki, D. L. (1990). Coronavirus transcription: Subgenomic mouse hepatitis virus replicative intermediates function in RNA synthesis. *Proc. Natl. Acad. Sci. USA* **64,** 1050–1056.

Sawicki, S. G., and Sawicki, D. L. (1995). Coronaviruses use discontinuous extension for synthesis of subgenome-length negative strands. *In* "Corona- and Related Viruses" (P. J. Talbot and G. A. Levy, Eds.), pp. 499–506. Plenum, New York.

Sethna, P. B., Hung, S. L., and Brian, D. A. (1989). Coronavirus subgenomic minus-strand RNAs and the potential for mRNA replicons. *Proc. Natl. Acad. Sci. USA* **86,** 5626–5630.

Shi, S. T., Schiller, J. J., Kanjanahaluethai, A., Baker, S. C., Oh, J. W., and Lai, M. M. C. (1999). Colocalization and membrane association of murine hepatitis virus gene 1 products and de novo-synthesized viral RNA in infected cells. *J. Virol.* **73,** 5957–5969.

Shieh, C. K., Lee, H. J., Yokomori, K., La Monica, N., Makino, S., and Lai, M. M. C. (1989). Identification of a new transcriptional initiation site and the corresponding functional gene 2b in the murine coronavirus RNA genome. *J. Virol.* **63,** 3729–3736.

Skinner, M. A., and Siddell, S. G. (1983). Coronavirus JHM: Nucleotide sequence of the mRNA that encodes nucleocapsid protein. *Nucleic Acids Res.* **11,** 5045–5054.

Smith, D. B., Johnson, K. S. (1988). Single-step purification of polypeptides expressed in *Escherichia coli* as fusions with glutathione *S*-transferase. *Gene* **67,** 31–40.

Spaan, W. J. M., Delius, H., Skinner, M., Armstrong, J., Rottier, P., Smeekens, S., van der Zeijst, B. A. M., and Siddell, S. G. (1983). Coronavirus mRNA synthesis involves fusion of non-contiguous sequences. *EMBO J.* **2,** 1839–1844.

Stohlman, S. A., Baric, R. S., Nelson, G. H., Soe, L. H., Welter, L. M., and Deans, R. J. (1988). Specific interaction between coronavirus leader RNA and nucleocapsid protein. *J. Virol.* **62,** 4288–4295.

Stohlman, S. A., and Lai, M. M. C. (1979). Phosphoproteins of murine hepatitis viruses. *J. Virol.* **32,** 672–675.

Yu, W., and Leibowitz, J. L. (1995). Specific binding of host cellular proteins to multiple sites within the 3′-end of mouse hepatitis virus genomic RNA. *J. Virol.* **69,** 2016–2023.

Zhang, X. M., Herbst, W., Kousoulas, K. G., and Storz, J. (1994a). Biological and genetic characterization of a hemagglutinating coronavirus isolated from a diarrhoeic child. *J. Med. Virol.* **44,** 152–161.

Zhang, X. M., and Lai, M. M. C. (1994). Unusual heterogeneity of leader-mRNA fusion in the murine coronavirus: Implications for the mechanism of RNA transcription and recombination. *J. Virol.* **68,** 6626–6633.

Zhang, X. M., and Lai, M. M. C. (1995). Interactions between the cytoplasmic proteins and the intergenic (promoter) sequence of murine hepatitis virus RNAs: Correlation with the amounts of subgenomic mRNA transcribed. *J. Virol.* **69,** 1637–1644.

Zhang, X. M., Li, H.-P., Xue, W., and Lai, M. M. C. Formation of a ribonucleoprotein complex of mouse hepatitis virus involving heterogeneous nuclear ribonucleoprotein A1 and transcription-regulatory elements of viral RNA. *Virology* **264,** 115–124.

Zhang, X. M., Liao, C. L., and Lai, M. M. C. (1994b). Coronavirus leader RNA regulates and initiates subgenomic mRNA transcription both in trans and in cis. *J. Virol.* **68,** 4738–4746.